Applied Soft Computing 50 (2017) 21–33

Contents lists available at ScienceDirect

Applied Soft Computing

journal homepage: www.elsevier.com/locate/asoc

Reservoir flood control operation using multi-objective evolutionary algorithm with decomposition and preferences

Yutao Qi[a,*], Jusheng Yu[a], Xiaodong Li[b], Yanxi Wei[a], Qiguang Miao[a]

[a] School of Computer Science and Technology, Xidian University, Xi'an, China
[b] School of Computer Science and IT, RMIT University, Melbourne, Australia

ARTICLE INFO

Article history:
Received 18 September 2015
Received in revised form 9 October 2016
Accepted 7 November 2016
Available online 11 November 2016

Keywords:
Reservoir flood control operation
Multi-objective evolutionary algorithm
MOEA/D
Preference

ABSTRACT

In this paper we propose a preference-based multi-objective optimization model for reservoir flood control operation (RFCO). This model takes the water preserving demand into consideration while optimizing two conflicting flood control objectives. A preference based multi-objective evolutionary algorithm with decomposition, named MOEA/D-PWA, is developed for solving the proposed RFCO model. For RFCO, it is challenging to define the preferred region formally, as the preference information is implicit and difficult to formulate. MOEA/D-PWA estimates the preferred region dynamically according to the final water level of solutions in the population, and then guides the search by propelling solutions towards the preferred region. Experimental results on four types of floods at the Ankang reservoir have illustrated that the suggested MOEA/D-PWA can successfully produce solutions in the preferred region of the Pareto front. The schedules obtained by MOEA/D-PWA can significantly reduce the flood peak and guarantee the dam safety as well. The proposed MOEA/D-PWA is also efficient in term of computational cost.

1. Introduction

Flood disaster is considered as one of the world's most common natural disasters. To reduce from flood damages, dams and reservoirs are constructed to regulate water flow and reduce flood peaks [1]. Reservoir flood control operation (RFCO) problem is a nonlinear non-convex optimization problem that involves multiple long-term and short-term objectives [2]. During the flood season, the safety of both upstream and downstream, which are conflict with each other, becomes the major problem in RFCO. Due to the conflict between objectives, the RFCO problem can be modeled as a multi-objective optimization problem (MOP) [3].

At present, most research works on RFCO transform the multi-objective optimization task into single-objective ones by combining multiple objectives using weighted sum methods [4,5], or choosing the primary criterion as the only objective while keeping the others as constraints [6,7]. The main shortcoming of these methods is that they often assume the weights are known a prior, and the solutions produced by these methods are not necessarily always the best trade-off solutions. Such problems could become even worse when joint schedule among multiple reservoir is required. Recently, more research efforts have been devoted to solving the original RFCO problem by using advanced multi-objective optimization techniques [8,9]. These approaches optimize the conflicting objectives in RFCO problem simultaneously and generate a set of trade-off solutions which are termed as non-dominated solutions to the multi-objective RFCO problem. Given a diverse set of candidate solutions, a decision maker can make a more informed decision on whether solution is the most appropriate one for a given situation.

Most existing multi-objective methods for solving RFCO problems attempt to obtain a set of trade-off solutions, either with or without any preference information. However, only selected solutions from this set will be finally chosen by the decision makers [10]. In the RFCO problem, non-dominated solutions, whose final upstream water levels at the end of operating horizon are close to the final target level, will be preferred by decision makers. The main challenge of incorporating preference information into multi-objective RFCO approaches is that the final upstream water level (FUWL) preference is difficult to articulate, neither in the objective space nor in the decision space of the MOP, by using existing preference representation techniques [11,12]. This paper proposes a new preference-based model for multi-objective RFCO problem by determining the preferred region in the objective space dynamically according to the FUWL preference information. This preference model is then combined with a decomposition based multi-objective evolutionary algorithm to guide the search towards the preferred region.

* Corresponding author.
E-mail address: qi_yutao@163.com (Y. Qi).

http://dx.doi.org/10.1016/j.asoc.2016.11.007
1568-4946/

With the advantage of obtaining a set of non-dominated solutions in a single run, multi-objective evolutionary algorithms (MOEAs) offers a significant advantage over traditional multi-criteria methods [13]. Since the pioneering work of Schaffer [14], a number of MOEAs have been developed. Recently, Zhang et al. combined conventional decomposition approaches with MOEAs, and developed the multi-objective evolutionary algorithm based on decomposition (MOEA/D) [15]. MOEA/D decomposes the target MOP into a number of scalar optimization sub-problems by using aggregation approaches and then optimizes them simultaneously by using an evolutionary algorithm. Research works have shown that MOEA/D can produce high-quality solutions on continuous and combinatorial problems [16]. It performs well on problems with complex Pareto-sets [17], and can be easily combined with preference information by dynamically adapting the decomposing weight vectors of scalar optimization sub-problems [18]. With a refined set of weight vectors, MOEA/D is able to focus its search efforts on the preferred region.

In this work, a multi-objective evolutionary algorithm with decomposition and preference, named MOEA/D-PWA, is developed for solving multi-objective RFCO problem. The main contributions of this work are as follows:

1. Considering the final upstream water level preference, a new preference-based model which determines the preferred region in the objective space dynamically is developed for multi-objective RFCO problem.
2. Based on the proposed preference model, a preference based weight adjustment method is developed and incorporated into the framework of MOEA/D to guide the search towards the preferred region, giving rise to he proposed MOEA/D-PWA for solving multi-objective RFCO problem.

The remainder of this paper is organized as follows. Section 2 summarizes existing works on multi-objective RFCO problem. Section 3 describes the multi-objective optimization model with preference for RFCO problem. Section 4 presents the proposed preference model. Section 5 introduces the preference based weight adjustment method under the framework of MOEA/D. Section 6 describes the workflow of the proposed MOEA/D-PWA. Section 7 verifies the effectiveness of MOEA/D-PWA and presents some discussions on it. Finally, Section 8 concludes this paper.

2. Related works on multi-objective RFCO

Reservoir flood control operation (RFCO) is a challenging problem that involves interdependent decision variables and multiple nonlinear objectives [19]. Due to the complexity of the water resource management system, there is no uniform model for RFCO problem. For a long time, the RFCO problem was modeled as single objective optimization problems for simplicity. Recently, there has been a growing interest in considering multiple objectives in RFCO problem simultaneously, owing to the great progress of multi-objective optimization techniques. Different from single objective optimizer, a multi-objective algorithm for RFCO problem optimizes the conflicting objectives in RFCO problem at the same time and generates a set of non-dominated solutions which provides the decision maker with more comprehensive information about the problem.

In the past few years, different multi-objective optimization models and optimizers for RFCO problem have been developed. Yu et al. [20] developed a fuzzy decision making system for multi-objective RFCO problem. Kim et al. [21] investigated the four interconnected reservoir operation problem at the Han River Basin and developed the multi-objective evolutionary algorithm to solve it. Using multi-objective genetic algorithm [22], Janga-Reddy et al. proposed their optimizer for RFCO problem at the Bhadra Reservoir. Nagesh-Kumar et al. [23] suggested an elitist-mutated particle swarm optimization algorithm to refine the reservoir operation policies. Baltar et al. [24] proposed a optimization model with four objectives for RFCO problem and developed an optimizer based on particle swarm optimization technique. Chang et al. [25] developed a multi-objective evolutionary algorithm to solve the RFCO problem in a parallel reservoir system in Taiwan. Based on the ant colony optimization algorithm, Afshara et al. [26] presented a multi-objective optimizer for refining the reservoir operating policy. Following the algorithmic workflow of shuffled frog leaping algorithm, Li et al. [27] proposed a multi-objective optimization algorithm for RFCO problem at the Three Gorges reservoir. Hakimi-Asiabara et al. [28] developed a genetic algorithm with self-learning for deriving optimal operating policies for three-objective multi-reservoir system. Qin et al. proposed a bi-objective optimization model for RFCO problem and then developed a cultured differential evolution algorithm [8] to solve it. Based on the artificial immune system and the character of multi-objective optimization problems in the decision space, Qi et al. [3] developed a multi-objective immune algorithm with Baldwinian learning for RFCO problem. Guo et al. [29] developed particle swarm optimization algorithm with a non-dominated sorting to handle the multi-reservoir operation problem. Zhou et al. [30] developed an integrated adaptive optimization model for derivation of multipurpose reservoir operating rule curves including ecological operating rule curve under future climate change which is predicted by a support vector machine model [31–34]. Ashkan et al. [35] incorporated artificial neural network into multi-objective evolutionary algorithm, giving rise to an optimizer to extract the best set of reservoir operation decisions.

At present, almost all of the existing algorithms for multi-objective RFCO problems were developed with the aim of obtaining a set of non-dominated solutions that approximates the entire Pareto front (PF) which is the whole set of the best trade-off solutions. Few works have been done on the study of incorporating decision maker's preference into multi-objective optimizers for RFCO problems, although the preference based multi-objective optimization is not new in the field of multi-criteria decision making [36]. Due to the complexity of RFCO problems, the difficulties of obtaining solutions at different PF regions could be various. In this case, multi-objective optimizers can hardly obtain a set of non-dominated solutions with good enough coverage on the PF, instead, they are likely to converge to different PF regions on different flood instances without control. On the other hand, it is time-consuming and unnecessary to approximate the entire PF, because only a small portion of solutions on PF are preferred by the decision maker. Therefore, this work focuses on how to represent the preference information specified by the decision maker, and how to incorporate the decision maker's preference into a decomposition based multi-objective optimizer to guide the search towards a preferred PF region.

3. Multi-objective model for RFCO problem

Considering the FUWL preference, the multi-objective model for RFCO problem can be mathematically described as follows [8,3].

In which, $\mathbf{Q}=(Q_1, Q_2, \ldots, Q_T)^T$ denotes the water release volumes at T scheduling periods. Each Q_t ($t=1, 2, \ldots, T$) must have a non-negative value no larger than its upper bound $Q_{\max}$. Z_t is the upstream water level of the tth scheduling period, it has a lower bound $Z_{\min}$ and a upper bound $Z_{\max}$. V_t and V_{t-1} are the reservoir storages of the tth and the $(t-1)$th scheduling period. I_t is the

reservoir's inflow volume of the tth scheduling period. Z_{FL} denotes the final target upstream water level at the end of the scheduling.

In Eq. (1), $f_1(\mathbf{Q})$ minimizes the highest upstream water level to guarantee the safety of the upstream side, while $f_2(\mathbf{Q})$ minimizes the largest water release volume to protect the downstream side. Constraints (1) and (2) define the value ranges of Z_t and Q_t. Constraints (3) is the water balance condition, according to which the upstream water level at the next scheduling period Z_{t+1} can be calculated by using V_t, I_t and Q_t.

$$\begin{aligned}
&\text{Minimize} \quad \mathbf{F}(\mathbf{Q}) = (f_1(\mathbf{Q}), f_2(\mathbf{Q}))\\
&\quad f_1(\mathbf{Q}) = \max(Z_t)\\
&\quad f_2(\mathbf{Q}) = \max(Q_t)\\
&\quad t = 1, 2, \ldots, T\\
&\text{Subject to:}\\
&\quad (1)\ \ Z_{\min} \le Z_t \le Z_{\max}\\
&\quad (2)\ \ 0 \le Q_t \le Q_{\max}\\
&\quad (3)\ \ V_t = V_{t-1} + I_t - Q_t\\
&\text{Preference:}\\
&\quad (4)\ \ Z_T \to Z_{FL}
\end{aligned} \tag{1}$$

The preference (4) is the FUWL preference which means the upstream water level Z_T at the end of operating horizon should be as close as possible to the final target level Z_{FL}. Here, Z_{FL} could be the flood control water level during the flood season or the normal pool level at the end of the flood season. It should be noted that the FUWL preference is not modeled as a constraint, mainly because it is not easy to specify the value range of Z_T for different flood instances. In addition, the definition of the preference region helps the proposed algorithm to explore in the objective space more efficiently.

In MOP, no unique solution could meet all the conflicting objectives. Instead, there exit some best trade-offs named Pareto optimal solutions. Given two feasible solutions, denoted as $\mathbf{x}_A$ and $\mathbf{x}_B$, to the target MOP with m objectives, x_A is said to dominate x_B, denoted by $x_A \prec x_B$, if $f_i(x_A) \le f_i(x_B)$ for all $i \in \{1, \ldots, m\}$, and there exists an $j \in \{1, \ldots, m\}$ that satisfies $f_j(x_A) < f_j(x_B)$. A feasible solution is called the Pareto optimal solution if there is no other feasible solution dominates it. The collection of all the Pareto optimal solutions in the decision space is termed as the Pareto set (PS) whose image in the objective space is called the Pareto front (PF). The main tasks of this work are to determine the preferred region on the PF according to preference information, and obtain a finite set of Pareto optimal solutions uniformly scattered within the preferred PF region.

4. The preference model for multi-objective RFCO problem

Most existing preference based MOEAs for benchmark [37] and real-world problems [38] mainly focus on how to handle the mutual dependence and priorities of objectives. Since the FUWL preference in RFCO problem can neither be formally defined in the objective space nor in the decision space, existing preference modeling methods [39,11,40] cannot be directly employed.

The main challenge of the preference modeling in RFCO problem is how to transform the implicit preference information into the objective space and determine the preferred PF region. According to our previous investigations on multi-objective RFCO problem [3], Pareto optimal solutions with similar final upstream water level are also located closely to each other in the objective space. Based on such observation, the following preference model is defined to identify a contiguous region on the PF as the preferred PF region.

Fig. 1 illustrates the ideal of the proposed preference model. It can be seen from Fig. 1(a) that the preferred region, denoted as $\mathbf{P}^{\mathrm{R}}$, can be determined by a middle point $\mathbf{M} = (M_1, M_2, \ldots, M_m)^T$ and a veto threshold vector $\mathbf{V} = (V_1, V_2, \ldots, V_m)^T$ according to the following Eqs. (2)–(5).

$$\mathbf{P}^{\mathrm{R}} = \left\{ \mathbf{x} \,\middle|\, \left| f_i(\mathbf{x}) - M_i \right| \le V_i, \quad \mathbf{x} \in \Omega, \quad i = 1, \ldots, m \right\} \tag{2}$$

$$\mathbf{M} = \left\{ \mathbf{x} \,\middle|\, \min \left\{ \left| FL(\mathbf{x}) - Z_{FL} \right| \right\}, \quad \mathbf{x} \in \mathbf{S}^{\mathrm{P}} \right\} \tag{3}$$

$$\mathbf{V} = \left\{ (V_1, V_2, \ldots, V_m) \,\middle|\, V_i = 1.2 \times \hat{V}_i \right\} \tag{4}$$

$$\hat{V}_i = \max_{\mathbf{x} \in \mathbf{S}^{\mathrm{P}}} \left\{ \left| f_i(\mathbf{x}) - M_i \right| \right\}, \quad (i = 1, 2, \ldots, m) \tag{5}$$

In Eq. (3), $FL(\mathbf{x})$ denotes the final upstream water level of the solution $\mathbf{x}$. Z_{PT} is a positive preference threshold provided by the decision maker. $\mathbf{S}^{\mathrm{P}}$ is the preferred non-dominated solution set, it contains three or more non-dominated solutions in the current population whose final upstream water levels lie in a range between $Z_{FL} - Z_{PT}$ and $Z_{FL} + Z_{PT}$.

As shown in Eq. (4), the veto threshold vector extends the calculated result by 20%. The motivation behind this extension is that $\mathbf{S}^{\mathrm{P}}$ might not always cover the whole preferred region, the extended veto threshold vector is expected to provide better coverage of preferred region. As shown in Fig. 1(b), the preferred region is slightly larger than that covered by solutions in $\mathbf{S}^{\mathrm{P}}$.

In order to rank the preference degree of solutions in the population, a measure of the preference level is defined for each solution according to the middle point $\mathbf{M}$ and the veto threshold vector $\mathbf{V}$. Note the preference level of the solution $\mathbf{x}$ as PL($\mathbf{x}$), it can be calculated by Eq. (6).

$$\mathrm{PL}(\mathbf{x}) = \sqrt{\sum_{i=1}^{m} \left(\frac{f_i(\mathbf{x}) - M_i}{V_i} \right)^2} \tag{6}$$

The preference level of solution $\mathbf{x}$ is determined by the Mahalanobis distance between the solution and the middle point $\mathbf{M}$. If PL($\mathbf{x}$) is smaller than 1, the solution is located at the preferred region.

5. The preference based weight adjustment method in MOEA/D

After determining the preferred region in the objective space, a preference based weight adjustment (PWA) method is then developed under the framework of MOEA/D [15]. The PWA method helps to guide the search of MOEA/D towards the preferred region, using the geometric relationship between the sub-problems' weight vectors and their optimal solutions under the Tchebycheff decomposition scheme.

Given a MOP with m optimization objectives $F(\mathbf{x}) = (f_1(\mathbf{x}), \ldots, f_m(\mathbf{x}))^T$, and a m-dimensional weight vector $\boldsymbol{\lambda} = (\lambda_1, \ldots, \lambda_m)^T$ ($\sum_{i=1}^{m} \lambda_i = 1$, $\lambda_i \ge 0$, $i = 1, \ldots, m$), the Tchebycheff decomposition approach converts the target MOP into the following scalar optimization problem in Eq. (7).

$$\min_{\mathbf{x} \in \Omega} \ g^{tc}\left(\mathbf{x} \,|\, \boldsymbol{\lambda}, \mathbf{z}^*\right) = \min_{\mathbf{x} \in \Omega} \max_{1 \le i \le m} \left\{ \lambda_i \left| f_i(\mathbf{x}) - \mathbf{z}_i^* \right| \right\} \tag{7}$$

In which, $\mathbf{z}^* = (z_1^*, \ldots, z_m^*)^T$ $(z_i^* < \min\{f_i(\mathbf{x}) | \mathbf{x} \in \Omega\}, i = 1, \ldots, m)$ is the ideal point. Using a set of determined weight vectors, MOEA/D [15] decomposes the target MOP into several scalar optimization sub-problems and then applies evolutionary algorithm to optimize them simultaneously. It has been proved that under mild conditions, for each Pareto optimal solution of the target MOP, noted as $\mathbf{x}^*$, there must be a weight vector $\boldsymbol{\lambda}^*$ that takes $\mathbf{x}^*$ as the optimal solution to the decomposed scalar optimization sub-problem using Tchebycheff approach and weight vector $\boldsymbol{\lambda}^*$ [41]. In other words, each optimal solution to Eq. (7) is a Pareto optimal solution to the target MOP. This illustrates the correctness of the decomposition based multi-objective optimization algorithms such as MOEA/D. By solving a set of scalar optimization

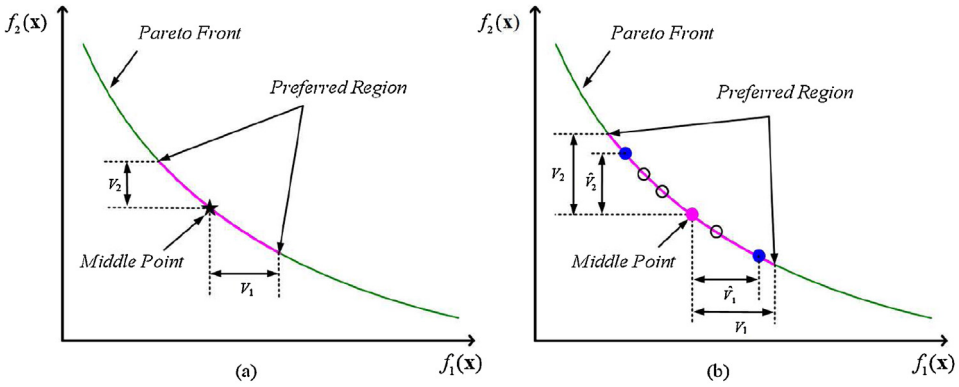

Fig. 1. The preference model based on irrigation demand.

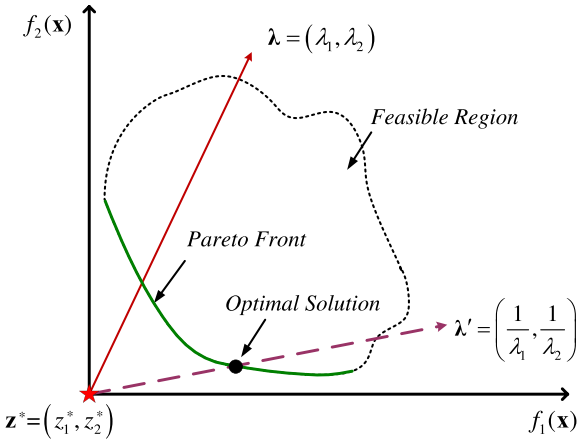

Fig. 2. Analysis on the Tchebycheff decomposition approach.

sub-problems in Eq. (7) with different weight vectors, MOEA/D can obtain a set of non-dominated solutions with good diversity [42].

In our previous work [43], we investigated the Tchebycheff decomposition scheme and discovered the following geometric relationship between the sub-problems' weight vectors and their optimal solutions. Fig. 2 takes a bi-objective problem for example to illustrate our previous findings. We have proved in [43] that, if the vector $\boldsymbol{\lambda}' = (1/\lambda_1, 1/\lambda_2)$ passing through $\mathbf{z}^*$ has an intersection with the PF of the target MOP, then the intersection point is the optimal solution of the scalar optimization sub-problem in Eq. (7) with weight vector $\boldsymbol{\lambda} = (\lambda_1, \lambda_2)$ [43].

For convenience of discussion, we name the vector $\boldsymbol{\lambda}'$ as the solution mapping vector of the scalar optimization sub-problem with weight vector $\boldsymbol{\lambda}$ and define the following WS-transformation which maps the weight vector of a scalar sub-problem to its solution mapping vector.

$$\lambda' = WS(\boldsymbol{\lambda}) = \left(\frac{1/\lambda_1}{\sum_{i=1}^{m} 1/\lambda_i}, \ldots, \frac{1/\lambda_m}{\sum_{i=1}^{m} 1/\lambda_i}\right) \tag{8}$$

We have also proved in theory that $\boldsymbol{\lambda} = \mathrm{WS}(\boldsymbol{\lambda}') = \mathrm{WS}(\mathrm{WS}(\boldsymbol{\lambda}))$ [43]. In other words, the above defined WS-transformation is self-inverse. If we apply the WS-transformation to the solution mapping vector $\boldsymbol{\lambda}'$, we can obtain the weight vector $\boldsymbol{\lambda}$. This is a useful mathematical property that will facilitate the development of this work.

Based on the analysis above, if we want to find some non-dominated solutions located within preferred PF region, we can first get the solution mapping vector $\boldsymbol{\lambda}'$ by using the ideal point $\mathbf{z}^*$ and the desired solution in the objective space, generate a new scalar optimization sub-problem with weight vector $\boldsymbol{\lambda} = \mathrm{WS}(\boldsymbol{\lambda}')$ thereafter, and then add it into the evolving population. This way, the algorithm will devote more computing efforts to sub-problems which are expected to find non-dominated solutions within the preferred PF region. This forms the core idea of the proposed MOEA/D-PWA.

6. The proposed MOEA/D-PWA

With the definition of the preferred region in the objective space, the proposed MOEA/D-PWA guides the search towards the preferred PF region by replacing scalar sub-problems from unwanted PF areas with new ones into the preferred region. During iterations, MOEA/D-PWA maintains the following items:

1. An evolving population with N individuals $evol\_pop = \{ind^1, \ldots, ind^N\}$, and $ind^i = \{\mathbf{x}^i, FV^i\}$, $i = 1, 2, \ldots, N$, where $\mathbf{x}^i$ is the current solution to the ith scalar sub-problem and $FV^i = F(\mathbf{x}^i)$.
2. A set of weight vectors for scalar sub-problems $\Lambda = \{\boldsymbol{\lambda}^1, \ldots, \boldsymbol{\lambda}^N\}$, and a neighborhood list $\mathbb{B} = \{\mathbf{B}(1), \mathbf{B}(2), \ldots, \mathbf{B}(N)\}$ for each sub-problem.
3. An estimated ideal point $\mathbf{z}^* = (z_1^*, \ldots, z_m^*)$, where z_i^* is slightly smaller than the best value obtained so far for the ith objective.
4. An external population EP for the storage of non-dominated solutions during the search.

MOEA/D-PWA requires a set of parameters as input, including the evolving population size N, the external population size N^E, the neighborhood size T, the initial middle point $\mathbf{M}^0$ and veto threshold vector $\mathbf{V}^0$, the maximal number of adjusted scalar sub-problems N^{WA}, the iteration interval of weight adjustment I^{WA}, and the maximal function evaluation number FE_{max}.

Given these parameters, the workflow of the proposed MOEA/D-PWA can be summarized in Algorithm 1.

Algorithm 1. The workflow of MOEA/D-PWA

Input: A stopping criterion: FE_{max}.
The parameters: N, N^E, T, $\mathbf{M}^0$, $\mathbf{V}^0$, N^{WA}, I^{WA}.
Output: $\{\mathbf{x}^1, \mathbf{x}^2, \ldots, \mathbf{x}^N\}$ and $\{FV^1, FV^2, \ldots, FV^N\}$;
1: $[\Lambda, \mathbb{B}, evol\_pop, \mathbf{z}^*, EP, \mathbf{M}, \mathbf{V}] \leftarrow$ **Initialization**$(N, T, \mathbf{M}^0, \mathbf{V}^0)$;
2: $gen \leftarrow 0$;
3: **While** Function evaluations $< FE_{max}$ **do**
4: $[evol\_pop, \mathbf{z}^*] \leftarrow$ **Evolving**();
5: $EP \leftarrow$ **UpdateEP**$(EP, evol\_pop, N^E)$;
6: $[\mathbf{M}, \mathbf{V}, \mathbf{S}^P] \leftarrow$ **UpdatePreferredRegion**(EP);
7: **If** $|EP| \geq N$ and $|\mathbf{S}^P| > 2$ and $gen \bmod I^{WA} = 0$ **do**
8: $[\Lambda, \mathbb{B}, evol\_pop] \leftarrow$ **RemoveSubproblems**$(N^{WA}, \mathbf{M}, \mathbf{V})$;
9: $[\Lambda, \mathbb{B}, evol\_pop] \leftarrow$ **AddNewSubproblems**$(N^{WA}, \mathbf{M}, \mathbf{V})$;
10: **End If**
11: $gen \leftarrow gen + 1$.
12: **End While**
13: **Return** $\{\mathbf{x}^1, \mathbf{x}^2, \ldots, \mathbf{x}^N\}$ and $\{FV^1, FV^2, \ldots, FV^N\}$.

The initialization step in MOEA/D-PWA (line 1) performs the following procedures. (1) Generate a set of evenly scattered weight vectors $\Lambda = \{\boldsymbol{\lambda}^1, \boldsymbol{\lambda}^2, \ldots, \boldsymbol{\lambda}^N\}$ for the N scalar sub-problems in *evol_pop*. (2) Establish a neighborhood list with size T for each sub-problem using the same method as in [15]. (3) Initialize individuals in *evol_pop* by generating $\mathbf{z}^* = (z_1^*, z_2^*, \ldots, z_m^*)$ at random, evaluate them and set $FV^i = \mathbf{F}(\mathbf{x}^i)$. (4) Determine the estimated ideal point $\mathbf{z}^* = (z_1^*, z_2^*, \ldots, z_m^*)$ by setting $z_i^* = \min\{f_i(\mathbf{x}^1), \ldots, f_i(\mathbf{x}^N)\} - 10^{-7}$. (5) Initialize the external population *EP* as empty set. (6) Set the initial middle point and veto threshold vector of the preferred region as their initial values $\mathbf{M}^0$ and $\mathbf{V}^0$.

The evolving step (line 4) generates new offsprings using the simulated binary crossover and the polynomial mutation, evaluate them, then update the solutions of sub-problems and the ideal point. This step is exact the same as that in the original MOEA/D algorithm [15].

The UpdateEP step (line 5) identifies the non-dominated solution set *NS* from the union set of current *EP* and *evol_pop*. If the size of *NS* is no larger than N^E, then let $EP := NS$. Otherwise, calculate the preference level of each solution in *NS* according to Eq. (6), then update *EP* by the solutions with the first N^E smallest preference levels in *NS*.

The UpdatePreferrdRegion step (line 6) choose the preferred Pareto optimal solutions whose preference levels are smaller than 1 from *EP* to form the population S^P. If S^P has three or more individuals, then update the middle point $\mathbf{M}$ and the veto threshold vector $\mathbf{V}$ according to Eqs. (3) and (4) respectively.

The preference based weight adjustment (PWA) steps (lines 8 and 9) are carried out when all the following three conditions hold at the same time. Firstly, *EP* has no less than N individuals. Secondly, the population S^P contains two or more preferred Pareto optimal solutions that satisfy Eq. (2). Finally, *gen* is divisible by I^{WA}. The PWA steps adjusts the weights of scalar sub-problems periodically by removing N^{WA} sub-problems from unwanted PF regions and adding the same amount of sub-problems into the preferred PF region. The details of the RemoveSubproblems and the AddNewSubproblems steps are respectively described in the following Algorithms 2 and 3.

In Algorithm 2, N^{WA} scalar sub-problems that preferred the least by the decision maker will be removed from the population according to the preferred PF region determined by $\mathbf{M}$ and $\mathbf{V}$. P^{NW} records the indices of sub-problems outside the preferred PF region. If the cardinality of P^{NW} is larger than N^{WA}, then the top N^{WA} sub-problems with largest value of preference level will be removed from the evolving population. Otherwise, all the sub-problems listed in P^{NW} will be removed at first, and then another $N^{WA} - |P^{NW}|$ ones with smallest crowding distances in the remaining population will also be removed.

Algorithm 2. $[\Lambda, \mathbb{B}, evol\_pop] \leftarrow$ **RemoveSubproblems**$(N^{WA}, \mathbf{M}, \mathbf{V})$

1: $P^{NW} \leftarrow$ *Empty set*;
2: **For** each $\mathbf{x}^i \in evol\_pop$ $(i = 1, 2, \ldots, N)$ **do**
3: $pl \leftarrow \mathrm{PL}\left(\mathbf{x}^i\right)$; //Using $\mathbf{M}$ and $\mathbf{V}$, according to Eq. (6).
4: **IF** $pl > 1$ **Then do** $P^{NW} \leftarrow P^{NW} \cup \{(i, pl)\}$;
5: **End For**
6: **IF** $|P^{NW}| > N^{WA}$ **Then do**
7: *DescendingSort*(P^{NW});
8: $[\Lambda', \mathbb{B}', evol\_pop'] \leftarrow Remove(P^{NW}[1, 2, \ldots, N^{WA}], \Lambda, evol\_pop)$;
9: **Otherwise do**
10: $[\Lambda', \mathbb{B}', evol\_pop'] \leftarrow Remove(P^{NW}, \Lambda, evol\_pop)$;
11: $[\Lambda', \mathbb{B}', evol\_pop'] \leftarrow RemoveCrowding(N^{WA} - |P^{NW}|, \Lambda', evol\_pop')$;
12: **End IF**
13: **Return** Λ', $\mathbb{B}'$ and $evol\_pop'$;

Algorithm 3. $[\Lambda, \mathbb{B}, evol\_pop] \leftarrow$ **AddNewSubproblems**$(N^{WA}, \mathbf{M}, \mathbf{V})$

1: $P^{EPF}, P^{ENW} \leftarrow$ *Empty set*;
2: **For** each $\mathbf{x}^j \in EP$ **do**
3: $pl \leftarrow \mathrm{PL}\left(\mathbf{x}^j\right)$; //Using $\mathbf{M}$ and $\mathbf{V}$, according to Eq. (6).
4: **IF** $pl < 1$ **Then do** $P^{EPF} \leftarrow P^{EPF} \cup \{(j, pl)\}$;
5: **Else** $P^{ENW} \leftarrow P^{ENW} \cup \{(j, pl)\}$;
6: **End For**
7: **IF** $|P^{EPF}| \geq N^{WA}$ **Then do**
8: **For** $i = 1, \ldots, N^{WA}$ **do**
9: $ind \leftarrow MostCrowingSolution(P^{EPF}, evol\_pop)$;
10: $P^{EPF} \leftarrow P^{EPF} - \{ind\}$;
11: $[\mathbf{x}^{new}, FV^{new}] \leftarrow CopyIndividual(EP, ind)$;
12: $\lambda^{new} \leftarrow \mathrm{WS}(FV^{new} - \mathbf{z}^*)$;
13: $[\Lambda', \mathbb{B}', evol\_pop'] \leftarrow AddSubproblem(\lambda^{new}, \mathbf{x}^{new}, FV^{new})$;
14: **End For**
15: **Otherwise do**
16: $[\Lambda', \mathbb{B}', evol\_pop'] \leftarrow AddSubproblems(|P^{EPF}|, P^{EPF})$;
17: $[\Lambda', \mathbb{B}', evol\_pop'] \leftarrow AddSubproblems(N^{\mathrm{WA}} - |P^{EPF}|, P^{ENW})$;
18: **End IF**
19: **Return** Λ', $\mathbb{B}'$ and $evol\_pop'$;

In Algorithm 3, N^{WA} preferred individuals in the external population *EP* are recalled into the evolving population and new weight vectors are generated and added to the sub-problem set. P^{EPF} and P^{ENW} respectively record the indices of sub-problems in *EP* within and outside the preferred PF region. If the cardinality of P^{EPF} is larger than N^{WA}, then calculate the crowding distance of individuals listed in P^{EPF} among *evol_pop*, pick up the top N^{WA} ones with largest crowding distance, and add these associated sub-problems into the evolving population *evol_pop*. Otherwise, add all the sub-problems listed in P^{EPF}, together with another $N^{WA} - |P^{EPF}|$ ones with smallest preference levels in P^{ENW} into *evol_pop*.

In conclusion, the PWA step removes scalar sub-problems outside the preferred PF region and adds new ones into the preferred area. It makes the algorithm devote more searching efforts to the preferred PF region and thus make efficient use of computing resources.

7. Experimental studies

In the experimental study, some typical floods at Ankang reservoir on the Hanjiang river in Shanxi Province of China are investigated. The Ankang reservoir was first built in October 1982 with an area of 77.5 km^2, and maximum water capacity of 2.585 billion cubic meters. It has a normal water level of 330 m, a flood control limit level of 325 m and a dead water level of 300 m. The Designed discharge capacity of Ankang reservoir is 37,474 m^3/s.

The parameters of the proposed MOEA/D-PWA are set as follows. The population size N is set to 20, the external population size N^E is set to 160, the neighborhood size T is set to 6, the initial middle point $\mathbf{M}^0$ = (325, 10,000) and veto threshold vector $\mathbf{V}^0$ = (2, 100), the maximal number of adjusted scalar sub-problems N^{WA} is set to 10, the iteration interval of weight adjustment I^{WA} is set to 20. The flood control limit level Z_{FL} is 325 m. The preference threshold Z_{PT} is set to different values to form different versions of MOEA/D-PWA. MOEA/D-PWA (1 m) and MOEA/D-PWA (2 m) represent the MOEA/D-PWA with the preference threshold of 1 m and 2 m respectively. More specifically, MOEA/D-PWA (1 m) will only find non-dominated solutions whose final upstream water level located between 324 m and 326 m. As for MOEA/D-PWA (2 m), the numbers of is between 323 m and 327 m.

The proposed MOEA/D-PWA is compared with the original MOEA/D [15], the well-known multi-objective evolutionary algorithm NSGAII [44], and the R-NSGA-II [39] algorithm which considers the decision maker's preference and incorporates the reference point based preference model into NSGA-II. To be fair, MOEA/D-PWA, MOEA/D, NSGAII and R-NSGA-II employ the same simulated binary crossover and polynomial mutation operators

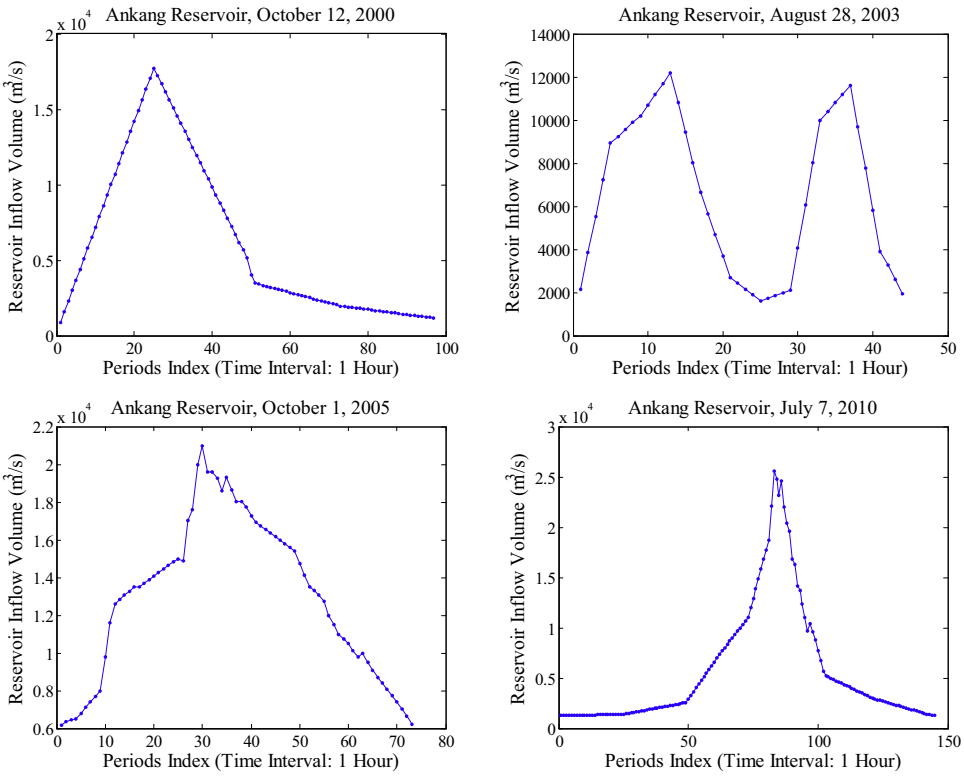

Fig. 3. Forecasted inflow volumes of floods at Ankang reservoir.

[44]. The population sizes of all the compared algorithms are set to 20. The stopping criteria for all comparing algorithms are that once each algorithm reaches the maximum number of function evaluations, which is 20,000, the algorithm is terminated. In view of the real time demand of the RFCO problem, the maximum function evaluation number cannot be too large. So, we set the population size to a relative small value.

7.1. The investigated floods

Four typical floods at the Ankang reservoir are selected as study cases in this work. Fig. 3 illustrates the forecasted reservoir inflow volumes of these four floods.

As shown in Fig. 3, floods on October 12, 2000, October 1st, 2005 and July 7, 2010 have one flood peak. The inflow volumes of these floods have different curve shape, maximum inflow volumes per second and total water volumes. Unlike these three floods, the flood on August 28, 2003 has two flood peaks with relatively low maximum inflow volumes per second.

7.2. Performance indicator

When dealing with a real world MOP, the true PF of the problem is usually unknown. At this situation, the hyper-volume (HV) indicator [45] is commonly used to evaluate the performance of the compared algorithms. In this work, only preferred non-dominated solutions are taken into consideration when calculating the HV indicator. Given a set of s preferred non-dominated solutions $\mathbf{P} = (\mathbf{p}_1, \mathbf{p}_2, \ldots, \mathbf{p}_s)$ for a minimization MOP and a reference point $\mathbf{R}^p$ in the m-dimensional objective space, the HV indicator is a measure of the region which is simultaneously dominated by the Pareto optimal solution set $\mathbf{P}$ and bounded above by the reference point $\mathbf{R}^p$. It can be formally described as the following Eq. (9), in which Volume$(\cdot)$ indicates the Lebesgue measure.

$$HV(\mathbf{P}, \mathbf{R}^p) = \mathbf{Volume}\left(\bigcup_{\mathbf{F}\in\mathbf{P}} \left\{x | \mathbf{F} \prec x \prec \mathbf{R}^p\right\}\right) \quad (9)$$

7.3. Effectiveness of the proposed MOEA/D-PWA

Taking the four typical floods as study cases, Figs. 6–13 illustrate the experimental results of the compared algorithms, which are the NSGAII [44], the MOEA/D [15], the R-NSGA-II [39] and the proposed MOEA/D-PWA with different preference thresholds respectively noted as MOEA/D-PWA (1 m) and MOEA/D-PWA (2 m).

The total scheduling times of floods on October 12, 2000, August 28, 2003, October 1st, 2005 and July 7, 2010 are 97 h, 44 h, 73 h and 145 h respectively. Their dispatching time intervals are set to 6 h, 3 h, 4 h, and 6 h to control the number of the decision variables. In order to make a better illustration of the algorithms' performance, an approximated Pareto front of each flood is taken as the baseline, we call it the ideal Pareto front. In these experimental studies, the ideal Pareto fronts of the four study cases are the non-dominated solution sets obtained by running NSGAII with 6,000,000 function evaluations over 30 runs.

Since R-NSGA-II is a preference based algorithm using the reference point based preference model, a reference point in the objective space should be specified by the decision maker in advance. In this part of experimental studies, the reference points for the four investigated floods in the years of 2000, 2003, 2005 and 2010 are set to (325, 6968), (325, 3884), (325, 12,345) and (325, 5827) respectively.

Fig. 4 illustrates the Pareto optimal solutions obtained by the compared algorithms for the flood on October 12, 2000. It can be seen that the non-dominated solutions found by MOEA/D cover a wider part of the ideal Pareto front than those obtained by NSGAII. However, the non-dominated solutions obtained by NSGAII cover the preferred PF region better than those obtained by MOEA/D,

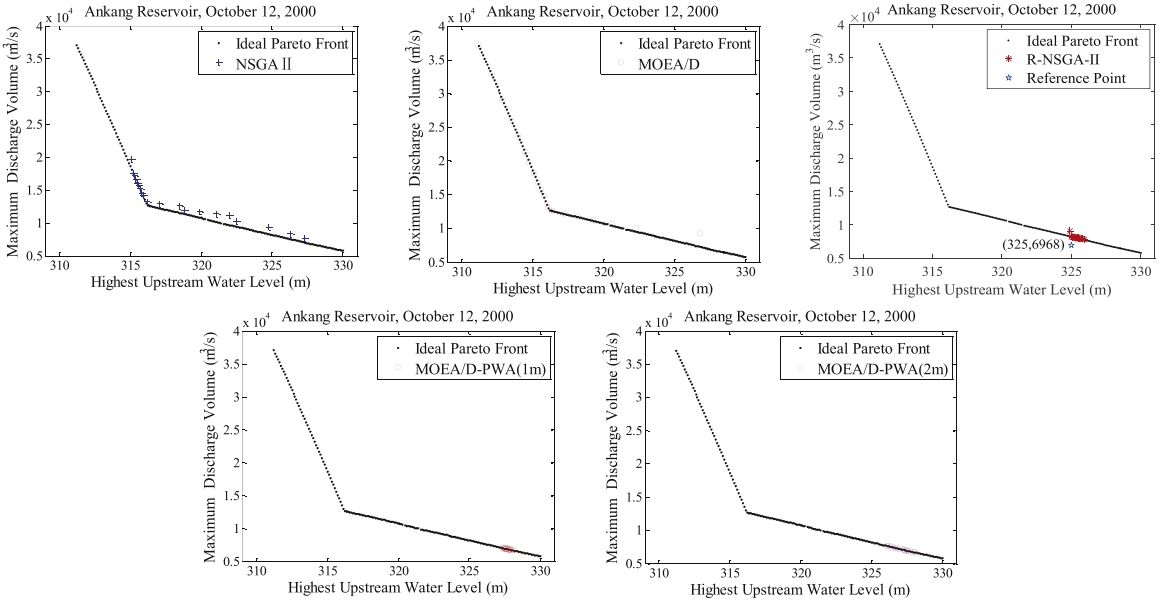

Fig. 4. Comparison of obtained non-dominated solutions for the flood on October 12, 2000. The ideal Pareto front is the non-dominated solution set obtained by running NSGAII with 6,000,000 function evaluations over 30 runs.

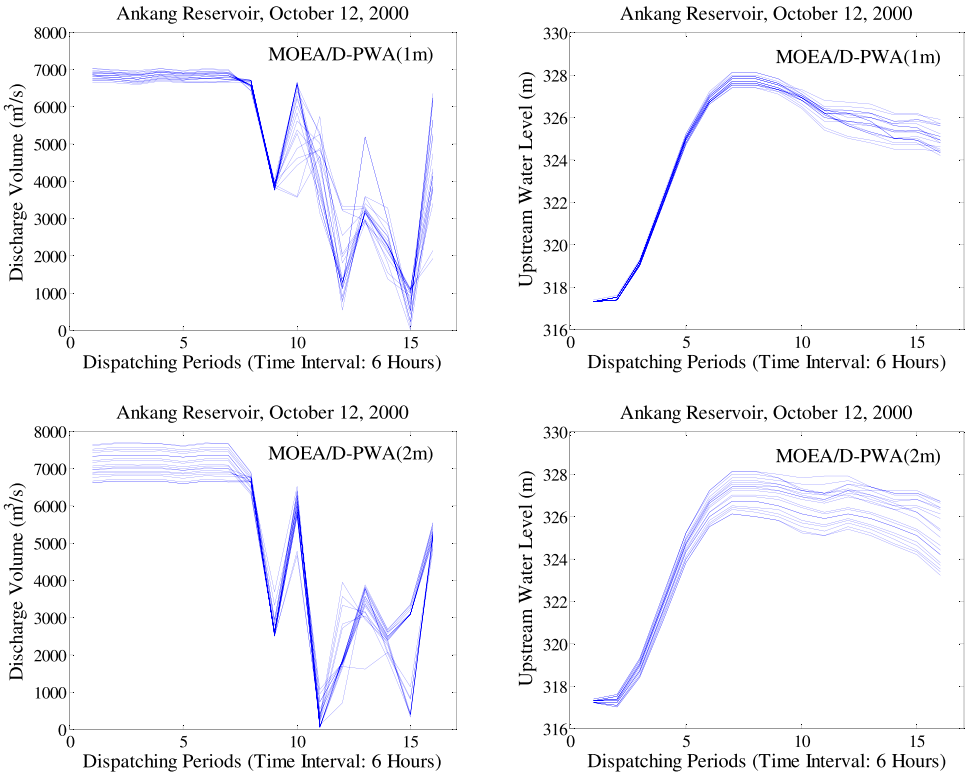

Fig. 5. Discharge volumes and the upstream water levels of the solutions obtained by MOEA/D-PWA (1 m) and MOEA/D-PWA (2 m) for the flood on October 12, 2000.

although they do not converge very well. That is to say, MOEA/D devotes a considerable amount of its computing efforts to the uninterested PF region. R-NSGA-II successfully converges to the PF region near the reference point as expected, however, it is not easy to specify an appropriate reference point in the objective space in advance. In this study case, the preferred PF region deviates from the point of (325, 6968), because the highest upstream water level is significantly higher than the final water level 325 m, as shown in Fig. 5. MOEA/D-PWA guides the search towards the preferred PF regions, as shown in Fig. 4, MOEA/D-PWA (1 m) and MOEA/D-PWA (2 m) successfully converge to their own preferred PF regions which are determined by the final water level preference information.

As shown in Fig. 5, the final upstream water levels of the schedules provided by MOEA/D-PWA (1 m) and MOEA/D-PWA (2 m) are located evenly within 1 m and 2 m above and below the flood control limit level of 325 m as expected. The solutions provided by MOEA/D-PWA (1 m) and MOEA/D-PWA (2 m) have their maximum discharging volumes less than 8000 m^3/s, which is less than half

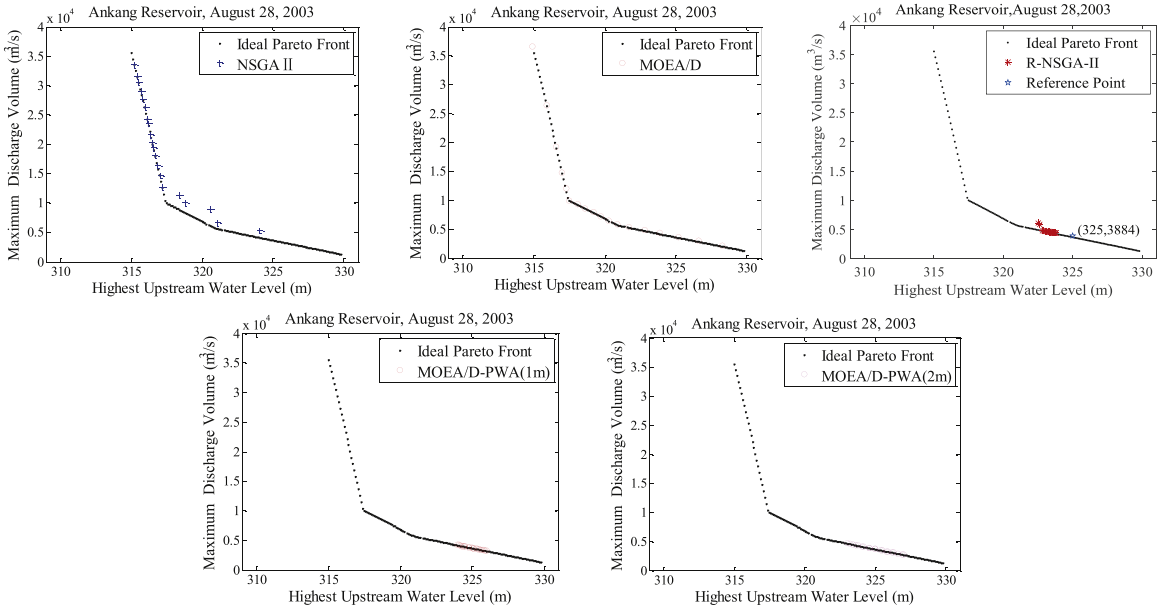

Fig. 6. Comparison of obtained non-dominated solutions for the flood on August 28, 2003. The ideal Pareto front is the non-dominated solution set obtained by running NSGAII with 6,000,000 function evaluations over 30 runs.

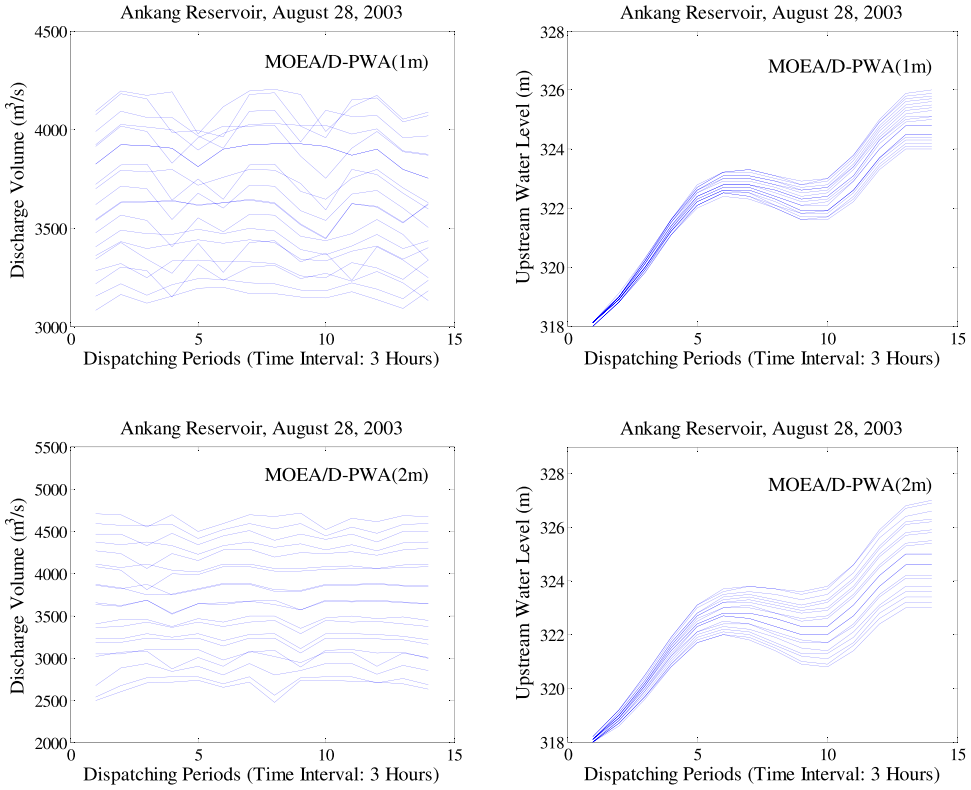

Fig. 7. Discharge volumes and the upstream water levels of the solutions obtained by MOEA/D-PWA (1 m) and MOEA/D-PWA (2 m) for the flood on August 28, 2003.

of the flood peak inflow volume 17,730 m^3/s. Thus, we can see that the proposed MOEA/D-PWA can provide solutions that significantly reduce the flood peak and the flood damages.

Figs. 6 and 7 illustrate the experimental results on the flood on August 28, 2003 which has two flood peaks and relatively low inflow volumes. As shown in Fig. 6, MOEA/D obtains a set of non-dominated solutions with better convergence, coverage and uniformity than those obtained by NSGAII. MOEA/D-PWA (1 m) and MOEA/D-PWA (2 m) also converge to different preferred PF regions. Moreover, MOEA/D-PWA (1 m) and MOEA/D-PWA (2 m) can provided solutions with stable discharge volumes, which keep the downstream free from the effect of the flood. As for the R-NSGA-II algorithm, it fails to converge to the preferred PF region specified by the reference point, mainly because it fails to generate good enough coverage before guiding the search towards the preferred PF region. It can be seen that even the NSGAII algorithm cannot obtain a satisfactory coverage over the preferred PF region within the allowed number of function evaluations.

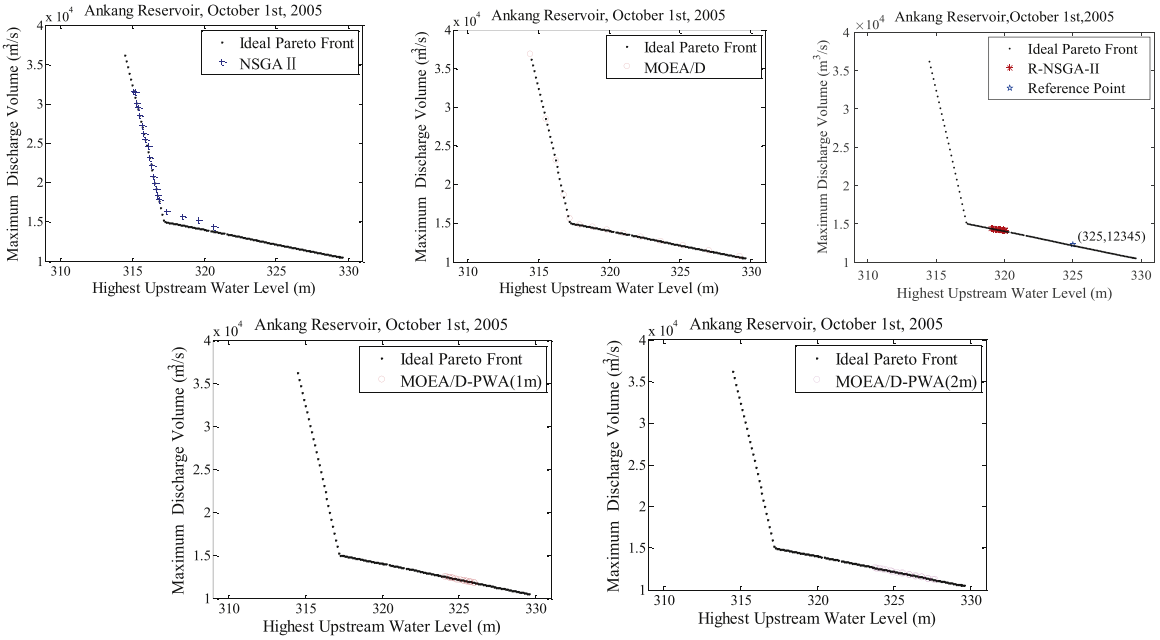

Fig. 8. Comparison of obtained non-dominated solutions for the flood on October 1st, 2005. The ideal Pareto front is the non-dominated solution set obtained by running NSGAII with 6,000,000 function evaluations over 30 runs.

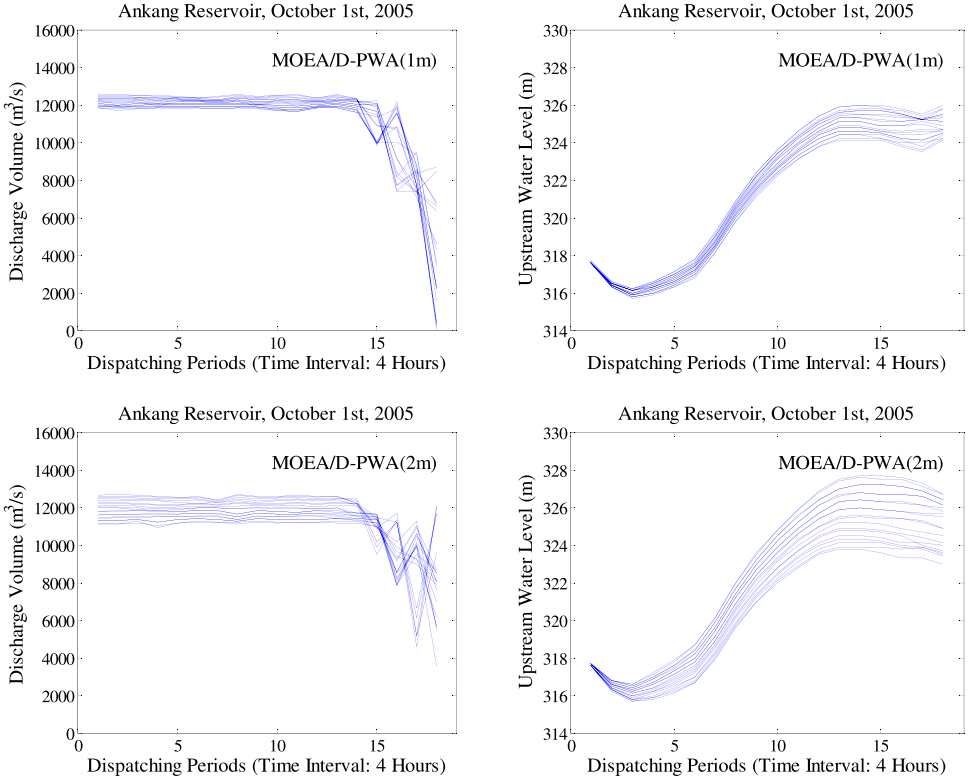

Fig. 9. Discharge volumes and the upstream water levels of the solutions obtained by MOEA/D-PWA (1 m) and MOEA/D-PWA (2 m) for the flood on October 1st, 2005.

Figs. 8 and 9 show the results on the flood on October 1st, 2005. This flood has one flood peak of 21,000 m^3/s and high total inflow water volume. Comparing the ideal PF in Fig. 8 with other problems shown in Figs. 4 and 6, this problem has a PF with sharp turning. Thus, at the preferred region, the performance on one objective deteriorates rapidly with the other one improves, which poses a big challenge to the optimization algorithms. From these two figures, we can observe that MOEA/D outperforms NSGAII. R-NSGA-II converges to a PF region far away from the reference point. MOEA/D-PWA successfully converges to the preferred PF region.

Figs. 10 and 11 illustrate the optimization results of the compared algorithms on the flood on July 7, 2010. For this flood with high and sudden peak of 25,537 m^3/s, NSGAII fails to obtain any non-dominated solution within the preferred PF region. Comparing with NSGAII, R-NSGA-II moves slightly towards the reference

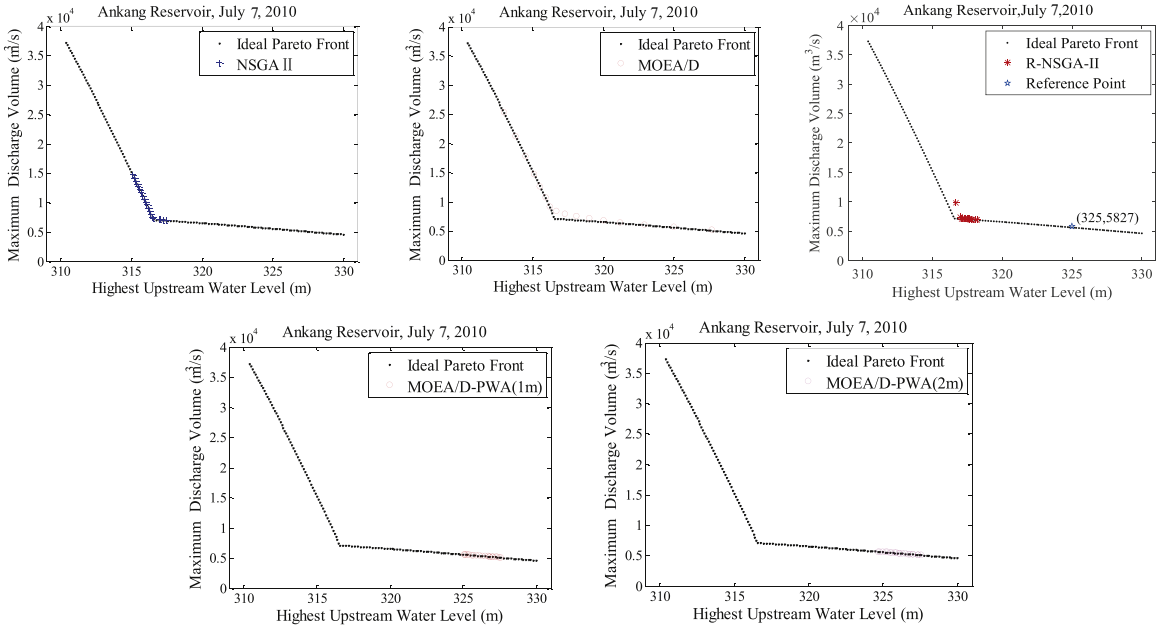

Fig. 10. Comparison of obtained non-dominated solutions for the flood on July 7, 2010. The ideal Pareto front is the non-dominated solution set obtained by running NSGAII with 6,000,000 function evaluations over 30 runs.

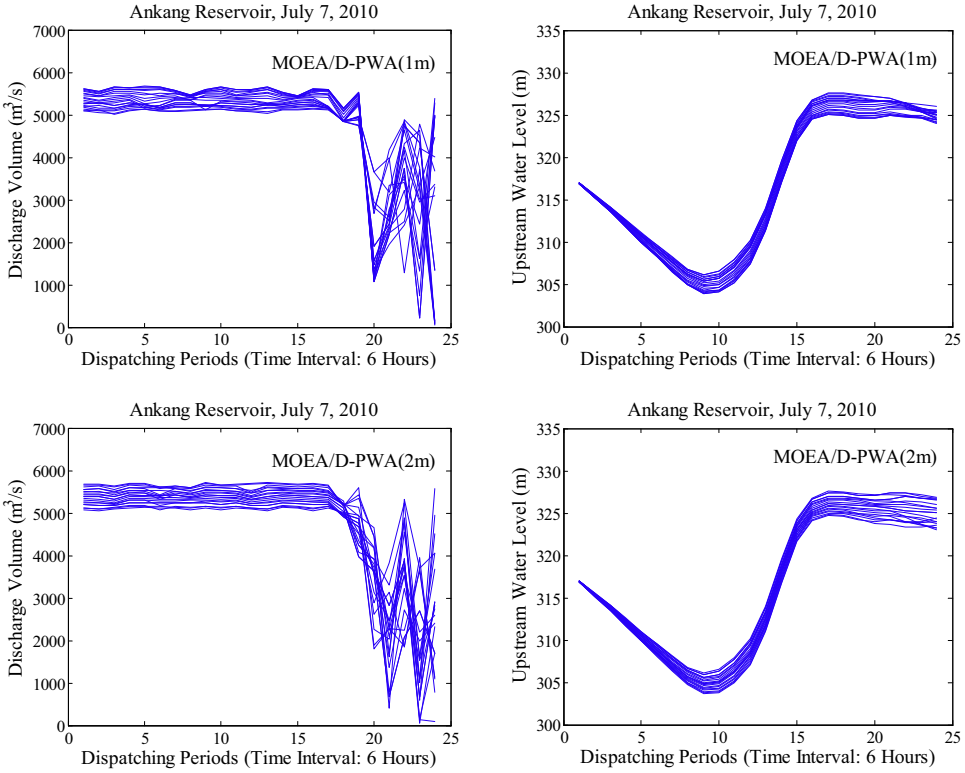

Fig. 11. Discharge volumes and the upstream water levels of the solutions obtained by MOEA/D-PWA (1 m) and MOEA/D-PWA (2 m) for the flood on July 7, 2010.

point along the PF cure, but it still fails to reach the preferred PF region. MOEA/D also performs well on this challenging problem, which indicates that this algorithm is efficient and suitable for solving multi-objective reservoir flood control operation problem. Following the framework of MOEA/D, the proposed MOEA/D-PWA successfully converges to the preferred PF region. In other words, MOEA/D-PWA can obtain more preferred solutions which will be finally adopted by the decision makers than MOEA/D.

To sum up, from above experimental investigations we can see that the non-dominated solutions obtained by NSGAII converge to different PF regions which are highly depend on the flood instances. MOEA/D has better coverage on the Pareto fronts than NSGAII, due to its good diversity preserving capability. R-NSGA-II is highly rely on the reference point specified by the decision maker, and it fails to converge to the PF regions near the reference points in some study cases. MOEA/D-PWA successfully converged to the preferred

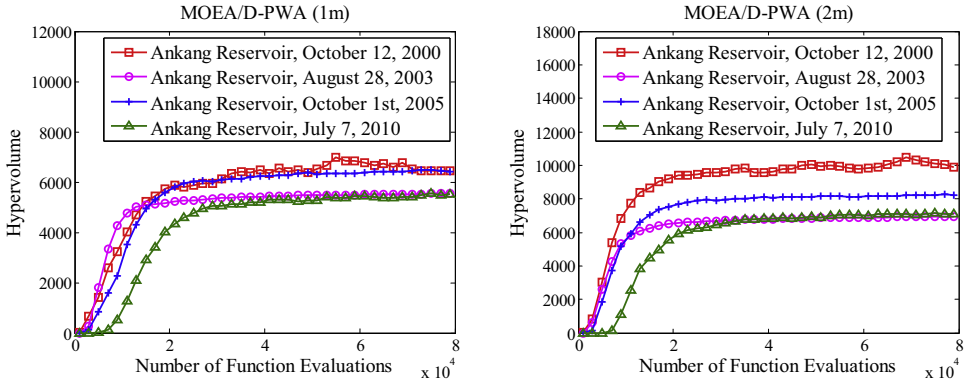

Fig. 12. Evolution of the average HV indicator of the preferred non-dominated solutions found by MOEA/D-PWA (1 m) (left) and MOEA/D-PWA (2 m) (right) on the four investigated floods.

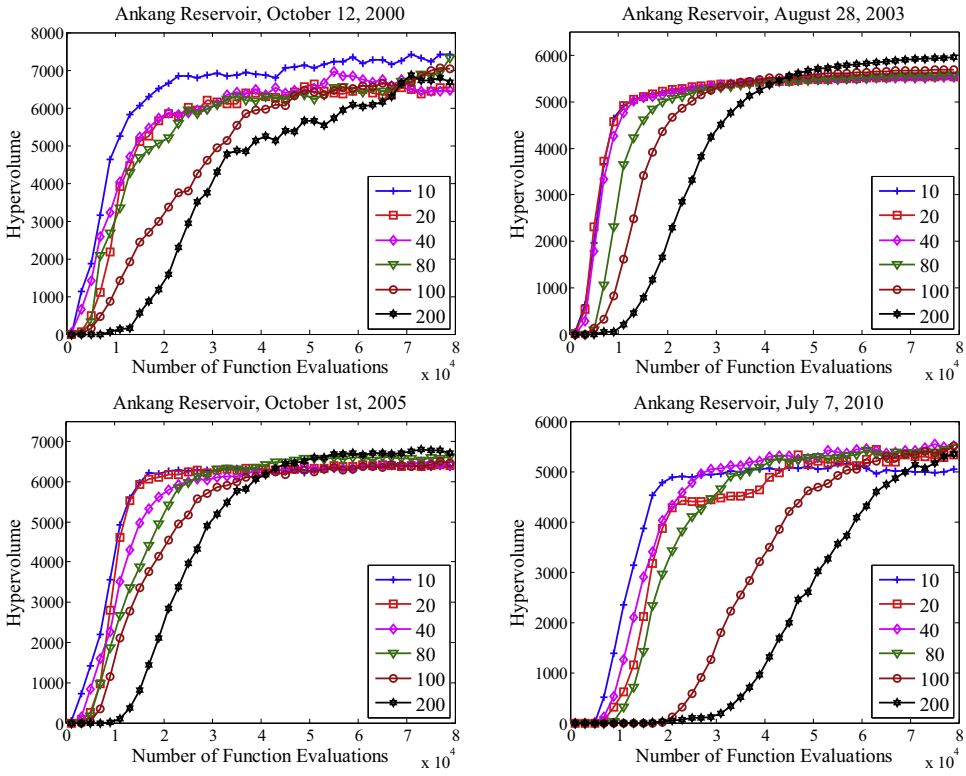

Fig. 13. Evolution of the average HV indicator of the preferred non-dominated solutions found by MOEA/D-PWA (1 m) on the investigated floods with different population size.

PF regions, it performs stably on the investigated problems and provides more preferred solutions to the decision makers.

7.4. Parametric studies

In the application of flood control, the decision maker usually wants to stop the algorithm as soon as possible and find the best trade-off between the quality of solutions and the speed of convergence. In this part of experimental studies, the two key parameters of the proposed MOEA/D-PWA are investigated. One parameter is the maximal function evaluation number FE^{max}, which determines when the algorithm will stop and give a set of non-dominated solutions with good enough quality. The other one is the evolving population size N, which determines how much computing effort is needed to evolve at each iteration.

In these experiments, the HV indicator is employed to evaluate the quality of the obtained non-dominated solution set. The reference points for calculating the HV values are set as follows, (330, 10,000) for the flood on October 12, 2000, (328, 5000) for the flood on August 28, 2003, (328, 14,000) for the flood on October 1st 2005 and (329, 7000) for the flood on July 7, 2010. It should be noted that only preferred non-dominated solutions are taken into consideration when calculating the HV values. Thus, the HV indicator becomes larger than zero until the preferred solutions appear. Experimental results in Figs. 12–14 are the averaged values of 30 independent runs.

Fig. 12 illustrates the evolution of the average HV indicator of the preferred non-dominated solutions found by MOEA/D-PWA (1 m) and MOEA/D-PWA (2 m) on the four investigated floods. As shown in this figure, all the HV curves climb up to relative stable values after the number of function evaluations reaches to about 20,000. Therefore, it is reasonable to conclude that 20,000 is an adequate value for the parameter FE^{max}.

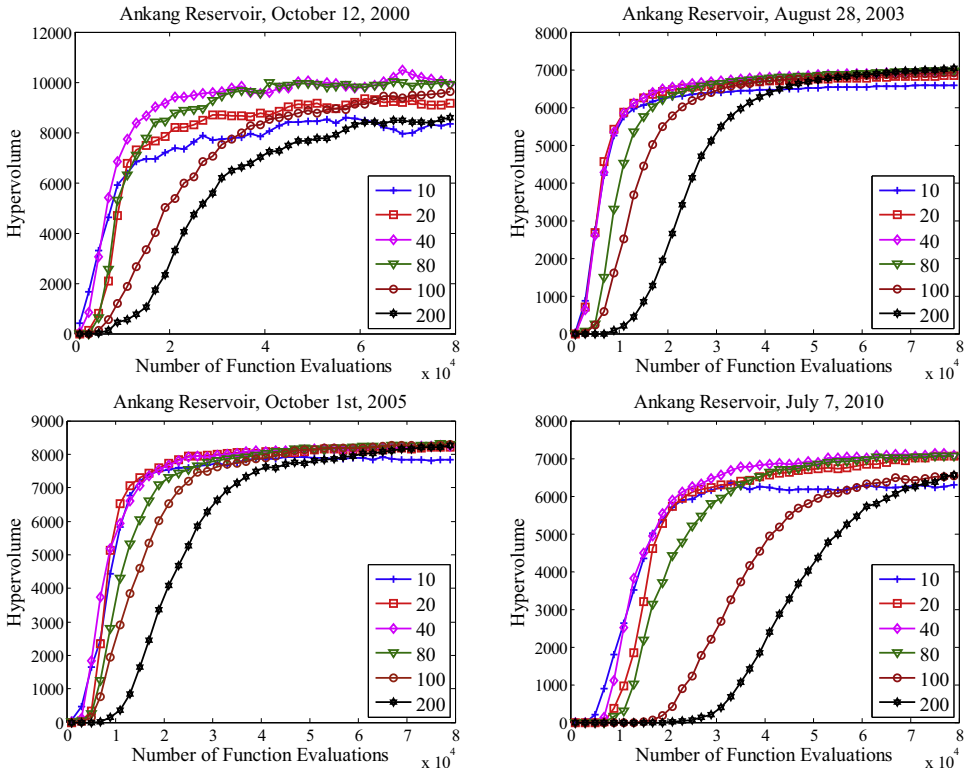

Fig. 14. Evolution of the average HV indicator of the preferred non-dominated solutions found by MOEA/D-PWA (2 m) on the investigated floods with different population size.

Figs. 13 and 14 illustrate the performances of MOEA/D-PWA (1 m) and MOEA/D-PWA (2 m) with different population size settings based on the HV indicator. In these figures, the ascending rates of the average HV curves indicate the convergence speed of implementations of MOEA/D-PWA with various population sizes. The final convergence values of the average HV curves illustrate the qualities of the non-dominated solution sets obtained by these implementations, the higher the better.

As shown in these Figs. 13 and 14, too large population size, 200 for example, will slow down the convergence rate of the algorithm, but the final HV values will be higher than other settings for some of the investigated floods (the floods on August 28, 2003 and October 1st, 2005). In contrast, small population size, 10 for example, will lead to a fast convergence, but the final HV values will not be as good as other settings. According to the experimental results in Figs. 13 and 14, it is a good choice to set the parameter of the population size between 20 and 80. In this work, the lower bound value 20 is employed.

8. Conclusions and future works

Reservoir flood control operation (RFCO) problem is a complex multi-objective optimization problem (MOP) that involves interdependent decision variables and multiple conflicting objectives. Due to its complexity, multi-objective optimizers can hardly obtain a set of non-dominated solutions with good enough coverage on the Pareto front (PF). Even worse, algorithms can converge to different PF regions on different flood instances without control. In order to guide the search of the multi-objective optimizer towards a specified PF region, a preference based multi-objective optimization algorithm is developed in this work for solving RFCO problem.

Although the ideal of incorporating decision maker's preference into multi-objective optimization algorithms is not new in the field of multi-criteria decision making, few works have been done on the preference based multi-objective optimizers for RFCO problems. Mainly because the final upstream water level (FUWL) preference in RFCO problem is implicit, it can be formulated neither in the objective space nor in the decision space by using existing preference representation techniques. In this work, a preference model for multi-objective RFCO problem is firstly developed by transforming the implicit preference information into the objective space. Thereafter, a modified MOEA/D algorithm incorporating preference based weight adjustment (MOEA/D-PWA) is proposed based on the suggested preference model. By replacing scalar sub-problems from unwanted PF areas with new ones into the preferred region, MOEA/D-PWA devotes more searching efforts to the preferred PF region and obtains more preferred non-dominated solutions.

Experimental studies on four typical floods at the Ankang reservoir have been done to verify the effectiveness of the preference model developed in this work. And with its help, the decomposition based multi-objective optimizer successfully converged to specified sub-region on the PF as we expected. The scheduling schemes obtained by MOEA/D- PWA can significantly reduce the flood peak and guarantee the dam safety as well.

Despite the effectiveness of MOEA/D-PWA, it can be further improved by employing an appropriate ideal point in the Tchebycheff decomposition approach to reduce the workload on the weight adjustment and increase the diversity of the decomposed sub-problems. How to determine an ideal point which is not far from and dominates the potential preferred PF region will be our future work.

Acknowledgements

This work was supported by the National Natural Science Foundation of China under Grant Nos. 61303119, 61472302 and 61272280.

References

[1] J.M.J. Schanze, E. Zeman (Eds.), Flood Risk Management: Hazards, Vulnerability and Mitigation Measures, Springer, 2006.
[2] B. Malekmohammadi, B. Zahraie, R. Kerachian, Ranking solutions of multi-objective reservoir operation optimization models using multi-criteria decision analysis, Expert Syst. Appl. 38 (6) (2011) 7851–7863.
[3] Y. Qi, F. Liu, M. Liu, M. Gong, L. Jiao, Multi-objective immune algorithm with Baldwinian learning, Appl. Soft Comput. 12 (8) (2012) 2654–2674.
[4] F. Wang, O. Saavedra Valeriano, X. Sun, Near real-time optimization of multi-reservoir during flood season in the Fengman Basin of China, Water Resour. Manag. 27 (12) (2013) 4315–4335.
[5] M. Hu, G.H. Huang, W. Sun, Y. Li, X. Ding, C. An, X. Zhang, T. Li, Multi-objective ecological reservoir operation based on water quality response models and improved genetic algorithm: a case study in Three Gorges Reservoir, China, Eng. Appl. Artif. Intell. 36 (2014) 332–346.
[6] S.K. Jain, G.N. Yoganarasimhan, S.M. Seth, A risk-based approach for flood control operation of a multipurpose reservoir, J. Am. Water Resour. Assoc. 28 (6) (1992) 1037–1043.
[7] L.-C. Chang, Guiding rational reservoir flood operation using penalty-type genetic algorithm, J. Hydrol. 354 (1–4) (2008) 65–74.
[8] Y.H.L.H. Qin, J.Z. Zhou, Y.L. Lu, Y.C. Zhang, Multi-objective cultured differential evolution for generating optimal trade-offs in reservoir flood control operation, Water Resour. Manag. 24 (2010) 2611–2632.
[9] Y. Qi, L. Bao, Y. Sun, J. Luo, Q. Miao, A memetic multi-objective immune algorithm for reservoir flood control operation, Water Resour. Manag. (2016) 1–21.
[10] J. Luo, C. Chen, J. Xie, Multi-objective immune algorithm with preference-based selection for reservoir flood control operation, Water Resour. Manag. 29 (5) (2015) 1447–1466.
[11] K. Deb, A. Kumar, Light beam search based multi-objective optimization using evolutionary algorithms, in: IEEE Congress on Evolutionary Computation, 2007, CEC 2007, 2007, pp. 2125–2132.
[12] R. Wang, R.C. Purshouse, I. Giagkiozis, P.J. Fleming, The iPICEA-g: a new hybrid evolutionary multi-criteria decision making approach using the brushing technique, Eur. J. Oper. Res. 243 (2) (2015) 442–453.
[13] A. Zhou, B.-Y. Qu, H. Li, S.-Z. Zhao, P.N. Suganthan, Q. Zhang, Multiobjective evolutionary algorithms: a survey of the state of the art, Swarm Evol. Comput. 1 (1) (2011) 32–49.
[14] J.D. Schaffer, Multiple objective optimization with vector evaluated genetic algorithms, in: Proceedings of the 1st International Conference on Genetic Algorithms, L. Erlbaum Associates Inc., Hillsdale, NJ, USA, 1985, pp. 93–100.
[15] Q. Zhang, H. Li, MOEA/D: a multiobjective evolutionary algorithm based on decomposition, IEEE Trans. Evol. Comput. 11 (6) (2007) 712–731.
[16] Y. Qi, Z. Hou, H. Li, J. Huang, X. Li, A decomposition based memetic algorithm for multi-objective vehicle routing problem with time windows, Comput. Oper. Res. 62 (2015) 61–77.
[17] H. Li, Q. Zhang, Multiobjective optimization problems with complicated Pareto sets, MOEA/D and NSGA-II, IEEE Trans. Evol. Comput. 13 (2) (2009) 284–302.
[18] A. Mohammadi, M. Omidvar, X. Li, Reference point based multi-objective optimization through decomposition, in: 2012 IEEE Congress on Evolutionary Computation (CEC), 2012, pp. 1–8.
[19] S. Hajkowicz, K. Collins, A review of multiple criteria analysis for water resource planning and management, Water Resour. Manag. 21 (9) (2007) 1553–1566.
[20] Y.-B. Yu, B.-D. Wang, G.-L. Wang, W. Li, Multi-person multiobjective fuzzy decision-making model for reservoir flood control operation, Water Resour. Manag. 18 (2) (2004) 111–124.
[21] T. Kim, J.H. Heo, Application of multi-objective genetic algorithms to multireservoir system optimization in the Han River basin, KSCE J. Civ. Eng. 10 (5) (2006) 371–380.
[22] M. Janga-Reddy, D. Nagesh-Kumar, Optimal reservoir operation using multi-objective evolutionary algorithm, Water Resour. Manag. 20 (6) (2006) 861–878.
[23] D. Nagesh-Kumar, M. Janga-Reddy, Multipurpose reservoir operation using particle swarm optimization, J. Water Resour. Plan. Manag. 133 (3) (2007) 192–201.
[24] A.M. Baltar, D.G. Fontane, Use of multiobjective particle swarm optimization in water resources management, J. Water Resour. Plan. Manag. 134 (3) (2008) 257–265.
[25] L.C. Chang, F.J. Chang, Multi-objective evolutionary algorithm for operating parallel reservoir system, J. Hydrol. 377 (1–2) (2009) 12–20.
[26] A. Afshara, F. Sharifiab, M.R. Jalaliab, Non-dominated archiving multi-colony ant algorithm for multi-objective optimization: application to multi-purpose reservoir operation, Eng. Optim. 41 (4) (2009) 313–325.
[27] Y.H. Li, J.Z. Zhou, Y.C. Zhang, H. Qin, L. Liu, Novel multiobjective shuffled frog leaping algorithm with application to reservoir flood control operation, J. Water Resour. Plan. Manag. 136 (2) (2010) 217–226.
[28] M. Hakimi-Asiabara, S.H. Ghodsypoura, KR, Deriving operating policies for multi-objective reservoir systems: application of self-learning genetic algorithm, Appl. Soft Comput. 10 (4) (2010) 1151–1163.
[29] X.N. Guo, T.S. Hu, C.L. Wu, T. Zhang, Y.B. Lv, Multi-objective optimization of the proposed multi-reservoir operating policy using improved NSPSO, Water Resour. Manag. 27 (7) (2013) 2137–2153.
[30] Y. Zhou, S. Guo, Incorporating ecological requirement into multipurpose reservoir operating rule curves for adaptation to climate change, J. Hydrol. 498 (2013) 153–164.
[31] B. Gu, V.S. Sheng, K.Y. Tay, W. Romano, S. Li, Incremental support vector learning for ordinal regression, IEEE Trans. Neural Netw. Learn. Syst. 26 (7) (2015) 1403–1416.
[32] B. Gu, X. Sun, V.S. Sheng, Structural minimax probability machine, IEEE Trans. Neural Netw. Learn. Syst. (99) (2016) 1–11, http://dx.doi.org/10.1109/TNNLS.2016.2544779.
[33] B. Gu, V.S. Sheng, A robust regularization path algorithm for v-support vector classification, IEEE Trans. Neural Netw. Learn. Syst. (99) (2016) 1–8, http://dx.doi.org/10.1109/TNNLS.2016.2527796.
[34] B. Gu, V.S. Sheng, Z. Wang, D. Ho, S. Osman, S. Li, Incremental learning for v-support vector regression, Neural Netw. 67 (2015) 140–150.
[35] S. Ashkan, OBH, A.M. Miguel, Multi-objective quantity-quality reservoir operation in sudden pollution, Water Resour. Manag. 28 (2) (2014) 567–586.
[36] L. Rachmawati, D. Srinivasan, Preference incorporation in multi-objective evolutionary algorithms: a survey, in: IEEE Congress on Evolutionary Computation, 2006. CEC 2006, 2006, pp. 962–968.
[37] R. Battiti, A. Passerini, Brain–computer evolutionary multiobjective optimization: a genetic algorithm adapting to the decision maker, IEEE Trans. Evol. Comput. 14 (5) (2010) 671–687.
[38] K.-B. Lee, J.-H. Kim, Multiobjective particle swarm optimization with preference-based sort and its application to path following footstep optimization for humanoid robots, IEEE Trans. Evol. Comput. 17 (6) (2013) 755–766.
[39] K. Deb, J. Sundar, UBRN, S. Chaudhuri, Reference point based multi-objective optimization using evolutionary algorithms, Int. J. Comput. Intell. Res. 2 (3) (2006) 635–642.
[40] Y. Jin, B. Sendhoff, Incorporation of Fuzzy Preferences Into Evolutionary Multiobjective Optimization, 2002.
[41] K. Miettinen, Nonlinear Multiobjective Optimization, Kluwer Academic Publishers, Boston, 1998.
[42] H. Ishibuchi, Y. Sakane, N. Tsukamoto, Y. Nojima, Simultaneous Use of Different Scalarizing Functions in MOEA/D, 2010.
[43] Y. Qi, X. Ma, F. Liu, L. Jiao, J. Sun, J. Wu, MOEA/D with adaptive weight adjustment, Evol. Comput. 22 (2) (2014) 231–264.
[44] K. Deb, A. Pratap, S. Agarwal, T. Meyarivan, A fast and elitist multiobjective genetic algorithm: NSGA-II, IEEE Trans. Evol. Comput. 6 (2) (2002) 182–197.
[45] E. Zitzler, L. Thiele, Multiobjective evolutionary algorithms: a comparative case study and the strength Pareto approach, IEEE Trans. Evol. Comput. 3 (4) (1999) 257–271.